

# Effect of neutrino rest mass on ionization equilibrium freeze-out

E. Grohs<sup>1</sup>, G. M. Fuller<sup>1</sup>, C. T. Kishimoto<sup>1,2</sup>, and M. W. Paris<sup>3</sup>

<sup>1</sup>*Department of Physics, University of California, San Diego, La Jolla, California 92093, USA*

<sup>2</sup>*Department of Physics, University of San Diego, San Diego, California 92110, USA and*

<sup>3</sup>*Theoretical Division, Los Alamos National Laboratory, Los Alamos, New Mexico 87545, USA*

(Dated: January 6, 2016)

We show how small neutrino rest masses can increase the expansion rate near the photon decoupling epoch in the early universe, causing an earlier, higher temperature freeze-out for ionization equilibrium compared to the massless neutrino case. This yields a larger free-electron fraction, thereby affecting the photon diffusion length differently than the sound horizon at photon decoupling. This neutrino-mass/recombination effect depends strongly on the neutrino rest masses. Though below current sensitivity, this effect could be probed by next-generation cosmic microwave background experiments, giving another observational handle on neutrino rest mass.

PACS numbers: 98.80.-k, 95.85.Ry, 14.60.Lm, 26.35.+c, 98.70.Vc

The history of the early universe is a history of freeze-outs, where reaction rates fall below the Hubble expansion rate. We point out here that the energy density associated with neutrino rest mass results in a subtle increase in the expansion rate at photon decoupling. This causes an earlier, higher temperature epoch for the freeze-out of ionization equilibrium. The physics of this freeze-out and its relation to observations of the cosmic microwave background (CMB) is a well studied issue [1–8]. The effect we consider, easily derivable with existing CMB analysis tools[9], has been mentioned[10] but not computed quantitatively. We find that these neutrino rest-mass induced changes in CMB observables are below the sensitivity of current methods used to observe and analyze the CMB data. The effects, however, may be within the reach of the next generation of precision CMB observations coupled with a self-consistent computational approach.

Here we focus on the influence of the recombination history on CMB observables, in particular the sound horizon  $r_s$  and the photon diffusion length  $r_d$ . The earlier ionization freeze-out caused by neutrino rest mass affects the deduced radiation energy density in a perhaps unexpected way. The quantities  $r_s$  and  $r_d$  are given in terms of integrals over the scale factor  $a$  [11]:

$$r_s = \int_0^{a_{\gamma d}} \frac{da}{a^2 H} \frac{1}{\sqrt{3(1+R)}}, \quad (1)$$

$$r_d^2 = \pi^2 \int_0^{a_{\gamma d}} \frac{da}{a^2 H} \frac{1}{a n_e(a) \sigma_T} \frac{R^2 + \frac{16}{15}(1+R)}{6(1+R)^2}, \quad (2)$$

where  $H = H(a)$  is the Hubble expansion rate,  $\sigma_T$  is the Thomson cross section,  $n_e(a)$  is the free-electron number density, and  $R(a) \equiv 3\rho_b/(4\rho_\gamma)$  is a ratio involving the baryon rest mass and photon energy densities,  $\rho_b$  and  $\rho_\gamma$ , respectively. The integrals span the early history of the universe, ending at  $a_{\gamma d}$ , the epoch of photon decoupling at a redshift  $z = 1090.43$  [11]. In the analysis to follow, we ignore the small dependence of the value of  $a_{\gamma d}$  on

$\sum m_\nu$ .<sup>1</sup> We should note that Eq. (2) is approximate and a more complete analysis would include effects beyond the tight-coupling approximation[12].

The photon diffusion length  $r_d$  depends on the number density of free electrons  $n_e^{(\text{free})}$ . The free-electron fraction,  $X_e \equiv n_e^{(\text{free})}/n_e^{(\text{total})}$ , parameterizes the free-electron number density. To evolve  $X_e$ , our recombination network uses the Saha equation to treat recombination onto He III and coupled Boltzmann equations

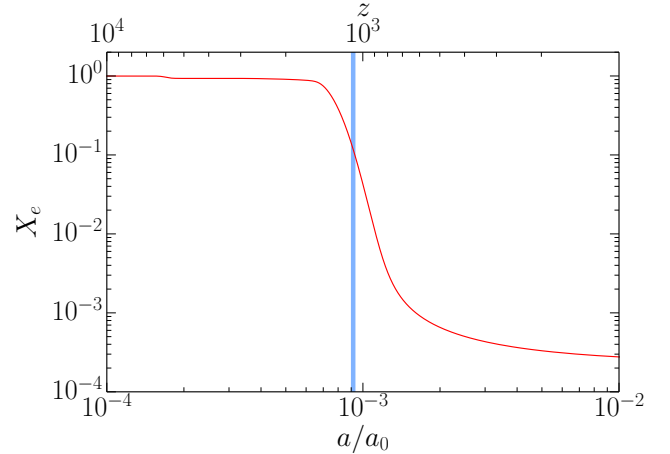


FIG. 1: (Color online.) The free-electron fraction,  $X_e$ , is given as a function of scale factor ratio,  $a/a_0$  ( $\equiv 1$  at current epoch), and redshift,  $z$ , (at top). The primordial helium mass fraction is taken to be  $Y_P = 0.242$ . Photon decoupling, denoted by the shaded, vertical bar, corresponds to the epoch as determined by Ref. [11].

<sup>1</sup> This is not entirely self-consistent but we will demonstrate that a consistent treatment changes the decoupling redshift from  $z = 1090$  to  $z = 1091$ . The associated change in  $a_{\gamma d}$  has negligible effect on  $r_s$  and  $r_d$ ; this is similar to the finding in Ref. [6].

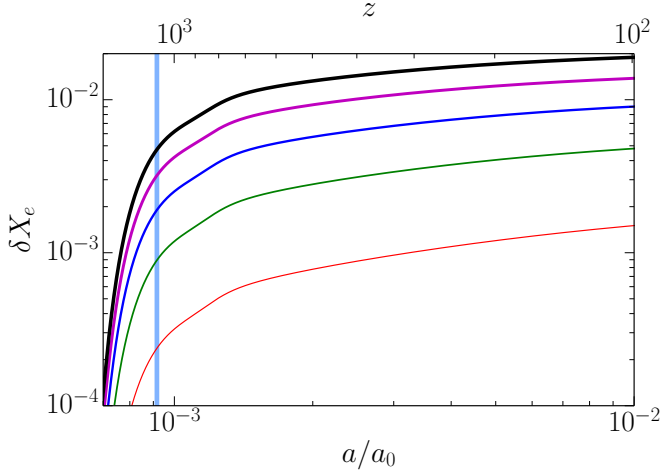


FIG. 2: (Color online.) The relative change in the free-electron fraction,  $\delta X_e = \Delta X_e / X_e$  given as a function of scale factor ratio,  $a/a_0$ , and redshift,  $z$ , (at top). The primordial helium mass fraction and vertical bar are identical to Fig. 1. Each curve corresponds to a different non-zero  $\sum m_\nu$ . The curves are in equal increments of  $\Delta \sum m_\nu = 0.2$  eV, starting with the smallest change for  $\sum m_\nu = 0.2$  eV and ending with the largest change for  $\sum m_\nu = 1.0$  eV.

[13, 14] to treat other recombination and ionization processes associated with H II, He II, and He III. We employ a recombination reaction network which is similar to, but independent of, the code `recfast`[15]. Figure 1 shows a calculation of the free-electron fraction as a function of scale factor ratio  $a/a_0$  ( $\equiv 1$  at current epoch), where we have taken  $\sum m_\nu = 0$ . Effects due to reionization processes at low redshift,  $z \sim \mathcal{O}(1)$  are neglected. The free-electron fraction of Fig. 1, evolved through the photon decoupling epoch, shows the freeze-out from ionization equilibrium. The first drop from the initial value of  $X_e = 1$  near  $a/a_0 \simeq 2 \times 10^{-4}$  is a consequence of the recombination onto He III.

In Fig. 2 we plot the change in  $X_e$  for non-zero values of  $\sum m_\nu$  relative to the case with  $\sum m_\nu = 0$ . Non-zero  $\sum m_\nu$  has a discernible effect on the freeze-out of  $X_e$ . A larger  $\sum m_\nu$  implies a larger Hubble rate giving an earlier epoch for  $X_e$  freeze-out. In a study of the expansion rate during recombination, Ref. [16] observed that scaling the Hubble rate affects the recombination history. Here we build on this argument to explicitly consider the role of neutrino rest mass on recombination. The curve describing the largest change corresponds to  $\sum m_\nu = 1.0$  eV, whereas the smallest change corresponds to  $\sum m_\nu = 0.2$  eV; consecutive curves are spaced by  $\Delta \sum m_\nu = 0.2$  eV.

Considering Eqs. (1) and (2) we note that both quantities,  $r_s$  and  $r_d$  depend on the expansion history  $H(a)$ . Only the diffusion length, however, depends explicitly on the recombination history  $n_e(a)$ , which is itself dependent on the expansion history. This recombination effect

changes  $r_d$  and this change is opposite to the effect of the change of that due directly to the Hubble expansion.

A scaling analysis, similar to that of Ref. [6], demonstrates the approximate relation between the sound horizon, the diffusion length, and the Hubble rate. Consider a scale transformation to the Hubble rate,  $H \rightarrow \lambda H$ , and the corresponding alteration to  $r_s$  and  $r_d$ . If we neglect the dependence of  $R(a)$  and  $n_e(a)$  on  $\lambda$  we have

$$r_s \propto \frac{1}{\lambda} \text{ and } r_d \propto \frac{1}{\sqrt{\lambda}} \implies \frac{r_s}{r_d} \propto \frac{1}{\sqrt{\lambda}}. \quad (3)$$

These relations suggest that a larger Hubble rate ( $\lambda > 1$ ) results in a smaller value of the ratio  $r_s/r_d$ . However, we show below that when the dependence of the recombination history  $n_e(a)$  on the expansion  $H(a)$  is taken into account  $r_s/r_d$  increases.

The radiation energy density is not directly measured by observation of the CMB. References [6] and [8], however, have shown that the ratio of the sound horizon to the photon diffusion length at the photon decoupling epoch is sensitive to the radiation energy density. Consequently, we distinguish between  $N_{\text{eff}}^{(\text{th})}$ , the input parameter that determines the radiation energy density in Eq. (4), and a measure of radiation energy density inferred from observations of the CMB, which we shall term  $\tilde{N}_{\text{eff}}$ . The theoretical definition of  $N_{\text{eff}}$  arises from the familiar parameterization of radiation energy density  $\rho_{\text{rad}}$  in terms of the photon temperature  $T(a)$  at decoupling  $T_\gamma \equiv T(a_{\gamma d})$  given by:

$$\rho_{\text{rad}} = \left(1 + \frac{7}{8} \left(\frac{4}{11}\right)^{4/3} N_{\text{eff}}^{(\text{th})}\right) \frac{\pi^2}{15} T_\gamma^4. \quad (4)$$

We adorn  $N_{\text{eff}}$  with a superscript (th) to distinguish the theoretical version of  $N_{\text{eff}}$ , an *input* parameter in public Boltzmann codes[9], from the CMB *inferred* value of  $N_{\text{eff}}$ ,  $\tilde{N}_{\text{eff}}$  described below. Calculations which include non-equilibrium processes in the early universe suggest  $N_{\text{eff}}^{(\text{th})} = 3.046$  [1, 3, 4, 17]. We determine  $\tilde{N}_{\text{eff}}$  by computing the sound horizon,  $r_s$  and the photon diffusion length,  $r_d$  at the photon decoupling epoch, as follows.

Active neutrinos decouple from the plasma with ultra-relativistic kinematics. As their occupation probabilities are comoving invariants thereafter, the energy density of non-degenerate neutrinos with rest masses  $m_{\nu_i}$  and neutrino temperature  $T_\nu$  is:

$$\begin{aligned} \rho_\nu(m_{\nu_i}, T_\nu) &= \sum_i \int \frac{d^3 p}{(2\pi)^3} E_i f_\nu(p, T_\nu) \\ &= \frac{1}{2\pi^2} \sum_i \int_0^\infty dp p^2 \frac{\sqrt{p^2 + m_{\nu_i}^2}}{e^{p/T_\nu} + 1}, \end{aligned} \quad (5)$$

where the sum is over active neutrino mass eigenstates,  $\nu_i$  and the second expression follows from an assumption of decoupled neutrinos, ignoring the small distortion due to irreversible neutrino transport effects. With

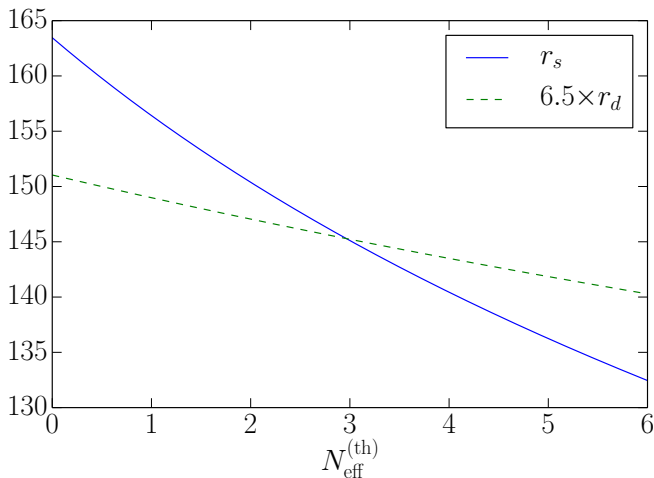


FIG. 3: (Color online.) The sound horizon  $r_s$  and diffusion length  $r_d$  as a function of  $N_{\text{eff}}^{(\text{th})}$ .

this assumption, the neutrino energy density for a given mass eigenstate is given by the product of the ultra-relativistic Fermi-Dirac occupation probabilities,  $f_\nu = (\exp(p/T_\nu) + 1)^{-1}$ , with the energy dispersion relation of a massive particle,  $E_i = \sqrt{p^2 + m_{\nu_i}^2}$ . Therefore, the energy density in the presence of a massive-neutrino species is larger than in the massless case and becomes increasingly significant at later times; it does not scale as  $T^4 \sim a^{-4}$  as in Eq. (4).

Using Eq. (6) with neutrino masses taken as described above for a given value of  $\sum m_\nu$  and the known relations for  $\rho_\gamma$  and  $\rho_b$  we compute the quantities  $r_s$  and  $r_d$  from Eqs. (1) and (2), respectively. We determine the inferred measure of  $N_{\text{eff}}$ ,  $\tilde{N}_{\text{eff}}$ , by choosing  $N_{\text{eff}}^{(\text{th})}$  in Eq. (4) to reproduce this ratio of  $r_s/r_d$ , which is a monotonically decreasing, invertible function of  $N_{\text{eff}}^{(\text{th})}$ ; see Fig. 3. The quantity  $\tilde{N}_{\text{eff}}$  reduces to  $N_{\text{eff}}^{(\text{th})}$  for massless, decoupled neutrinos. There is clearly no requirement that  $\tilde{N}_{\text{eff}}$  be independent of scale factor  $a$ . It has been motivated here by the need to characterize massive neutrinos but it is also applicable to non-standard cosmologies with constituents that may be far from equilibrium. Using the ratio  $r_s/r_d$  in the determination of  $\tilde{N}_{\text{eff}}$  avoids any reference to the angular diameter distance to last scattering and, therefore, dependence on the dark energy equation of state[6]. In contrast to Ref. [6] we do not change the value of the primordial helium abundance,  $Y_P$  to keep  $\theta_d$  fixed. This fact and  $\Delta(r_s/r_d) \sim -\Delta\tilde{N}_{\text{eff}}$  (since  $r_s/r_d$  is monotonically decreasing with  $\tilde{N}_{\text{eff}}$ ) means that a larger Hubble rate would imply a larger value of  $\tilde{N}_{\text{eff}}$ . In fact, as suggested in Fig. 2, the dependence of  $n_e(a)$  on the increased energy density from the neutrino rest mass dominates the explicit dependence on  $H(a)$  in Eq. (2). This has the consequence that a larger Hubble rate results in

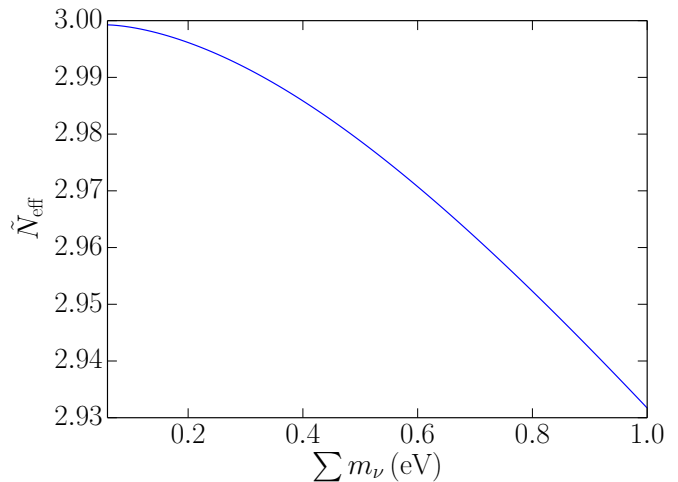


FIG. 4:  $\tilde{N}_{\text{eff}}$  as a function of  $\sum m_\nu$ . The minimum value for  $\sum m_\nu$  is  $\sim 0.06$  eV for the normal mass hierarchy.

a *larger* ratio of  $r_s/r_d$ ; see Figs. 4 to 6 and discussion below.

In order to investigate physics beyond the standard models of particle physics and cosmology, we have formulated a self-consistent approach that is not constrained to minimal extensions to the standard model. To do so, we simulate the early universe from weak decoupling through Big Bang Nucleosynthesis (BBN) to photon decoupling using the BURST code[18]. This treatment self-consistently incorporates binned, general, momentum occupation probabilities for each of six neutrino species ( $\nu_e$ ,  $\bar{\nu}_e$ ,  $\nu_\mu$ ,  $\bar{\nu}_\mu$ ,  $\nu_\tau$ , and  $\bar{\nu}_\tau$ ) and a Boltzmann treatment of neutrino scattering, absorption and emission processes to evolve the early universe.

In this treatment, neutrinos decouple from the  $\gamma$ ,  $e^\pm$  plasma at high temperatures,  $1 \lesssim T \lesssim 3$  MeV, with ultra-relativistic kinematics[19, 20] as expected. The computation of the helium abundance  $Y_P$  in this treatment however is more nuanced than in the standard cosmology. Here  $Y_P$  is not simply a function of  $N_{\text{eff}}^{(\text{th})}$  and  $\omega_b$ . Assuming zero lepton numbers and an adopted world-average neutron lifetime of 886 s, our calculations give a  $^4\text{He}$  primordial mass fraction  $Y_P = 0.242$  taking the baryon number  $\Omega_b h^2 \equiv \omega_b = 0.022068$  from the Ref. [11] best-fit. This is consistent with the observationally inferred primordial helium abundance [21, 22]. Although we take the neutrinos to decouple in weak eigenstates, i.e. flavor states, we write their occupation probabilities in the mass eigenbasis. Since we are assuming the neutrinos have identical thermal spectra with zero-chemical potential in the weak eigenstates, we can use the same occupation probabilities for the mass eigenstates at a given momentum  $p$ [19, 23].

Before considering the effect of the neutrino mass on  $\tilde{N}_{\text{eff}}$ , the deduced radiation energy density, we estimate

its effect on  $N_{\text{eff}}^{(\text{th})}$ . The cosmological constraint (at the level of  $2\sigma$ ) on the sum of the light neutrino masses is  $\sum m_\nu \leq 0.23$  eV [11]. If we take  $\sum m_\nu$  to be at this upper limit and assume degenerate mass eigenvalues, each neutrino has an associated mass  $\sim 0.08$  eV. We see that the neutrino rest masses and temperatures at photon decoupling ( $T_\gamma \approx 0.2$  eV,  $T_\nu \approx 0.15$  eV) are coincidentally at the same scale, meaning that neutrinos can not be treated either as pure matter or pure radiation. An individual neutrino has an average momentum of  $\sim 0.5$  eV at photon decoupling. As a consequence, we expect fractional corrections to the relativistic neutrino energy density stemming from neutrino rest mass to be  $\sim m^2/2p^2 \sim 0.01$ , with a concomitant change to  $N_{\text{eff}}^{(\text{th})}$  of  $\sim 3 \times 0.01 \sim +0.03$ . If we were to unphysically classify the entire neutrino energy density into  $\rho_{\text{rad}}$  the corresponding change to  $N_{\text{eff}}^{(\text{th})}$  would be  $\Delta N_{\text{eff}}^{(\text{th})} \equiv N_{\text{eff}}^{(\text{th})} - 3 \simeq \frac{5}{7\pi^2} \left(\frac{11}{4}\right)^{2/3} \sum_{i=1}^3 \left(\frac{m_i}{T_\gamma}\right)^2$ . We arrive then at  $\Delta N_{\text{eff}}^{(\text{th})} \simeq 0.04$  for  $\sum m_\nu = 0.23$  eV, a change consistent with the simple kinematic estimate above, and not to be confused with  $\Delta N_{\text{eff}}^{(\text{th})} \approx 0.046$  stemming from non-equilibrium neutrino scattering and quantum-electrodynamics effects inherent in Refs. [1–3].

Figure 4 shows  $\tilde{N}_{\text{eff}}$  versus  $\sum m_\nu$ . Contrary to the expectation of increased  $\tilde{N}_{\text{eff}}$  in our previous scaling and estimate arguments, we observe a monotonic decrease in  $\tilde{N}_{\text{eff}}$  with increasing  $\sum m_\nu$ . We denote this phenomenon the neutrino mass/recombination ( $\nu$ MR) effect. For illustrative purposes in Fig. 5, we treat  $\Delta\tilde{N}_{\text{eff}}$  as a quantity to be determined at any epoch, although  $N_{\text{eff}}$  is only

observed at photon decoupling. The neutrino rest mass has no discernible effect on  $\tilde{N}_{\text{eff}}$  at early epochs, at small  $a/a_0$ . At larger values of  $a/a_0$  ( $\sim 5 \times 10^{-4}$ ), the extra energy density from the neutrino rest masses produces a larger  $\tilde{N}_{\text{eff}}$  in accordance with Eq. (3). If we were to extrapolate this evolution trend to the epoch of photon decoupling, we would find a value of  $\Delta\tilde{N}_{\text{eff}} > 0$ . The  $\nu$ MR effect intervenes to modify this extrapolation and results in  $\Delta\tilde{N}_{\text{eff}} < 0$  at  $a_{\gamma d}$ .

Each evolution curve for  $\Delta\tilde{N}_{\text{eff}}$  in Fig. 5 corresponds to an evolution curve for  $X_e(a)$  in Fig. 2 for various values of  $\sum m_\nu$ . The smallest value of  $\sum m_\nu$  produces the smallest change in  $X_e$ , which subsequently changes  $\Delta\tilde{N}_{\text{eff}}$  the least. Conversely, the largest value of  $\sum m_\nu$  produces the largest change in  $X_e$ , which changes  $\Delta\tilde{N}_{\text{eff}}$  the most. From the curves in Fig. 5, it is clear that the effect of neutrino rest mass in producing a higher  $X_e$  at freeze-out overwhelms the effect of the extra energy density, thereby decreasing  $\tilde{N}_{\text{eff}}$  at photon decoupling, i.e. at  $a = a_{\gamma d}$ , the vertical bar in Figs. 2 and 5.

There are several interesting features to note in Fig. 5. Each curve in Fig. 5 goes through  $\Delta\tilde{N}_{\text{eff}} = 0$  near the value  $a/a_0 \sim (7.65 \pm 0.10) \times 10^{-4}$ . The larger the value of  $\sum m_\nu$ , the higher the curvature of the function  $\Delta\tilde{N}_{\text{eff}}(a)$ . For values of  $a/a_0$  above which  $\Delta\tilde{N}_{\text{eff}} = 0$ , the slope of  $\Delta\tilde{N}_{\text{eff}}(a)$  is a rapidly decreasing function of  $\sum m_\nu$ . We note that for  $\sum m_\nu = 0.23$  eV, the preferred upper limit from Ref. [11], we find  $\Delta\tilde{N}_{\text{eff}} = -0.005$ . This effect is certainly below present sensitivities of CMB observations. Next-generation CMB measurements, however, aspire to percent level accuracy in determinations of the relativistic energy density [24]. The exquisite sensitivity of the  $\nu$ MR effect on  $\Delta\tilde{N}_{\text{eff}}(a_{\gamma d})$  suggests that it may be an important component in future precision determinations of cosmological parameters.

As mentioned earlier, we do not constrain  $a_{\gamma d}$  to maintain a uniform optical depth  $\tau(a_{\gamma d})$

$$\tau(a_{\gamma d}) = \int_{a_{\gamma d}}^{a_0} \frac{da}{a^2 H} a n_e(a) \sigma_T \equiv 1, \quad (7)$$

when comparing different values for  $\sum m_\nu$ . Note that this definition of  $\tau(a_{\gamma d})$  does not include reionization effects on  $n_e(a)$ . We should emphasize that each curve in Figs. 2 and 5 is calculated using the same value for the scale factor of last scattering  $a_{\gamma d} = 9.162 \times 10^{-4}$  (corresponding to  $z = 1090.43$ ). This is not self consistent, strictly speaking, but we have verified that the effect on  $\tilde{N}_{\text{eff}}$ , due to the differences in  $n_e$  and  $H$ , is negligible. If we impose the constraint in Eq. (7), we find  $a_{\gamma d}$  decreases by a few parts in  $10^4$  for  $\sum m_\nu = 0.23$  eV, which has an insignificant effect on  $\tilde{N}_{\text{eff}}$ .

Up to this point in the present analysis we have not considered variation of the primordial helium mass fraction  $Y_P$  since BBN occurs at high enough temperatures that the neutrinos are effectively massless. If we consider, however, cosmological parameters that affect  $Y_P$

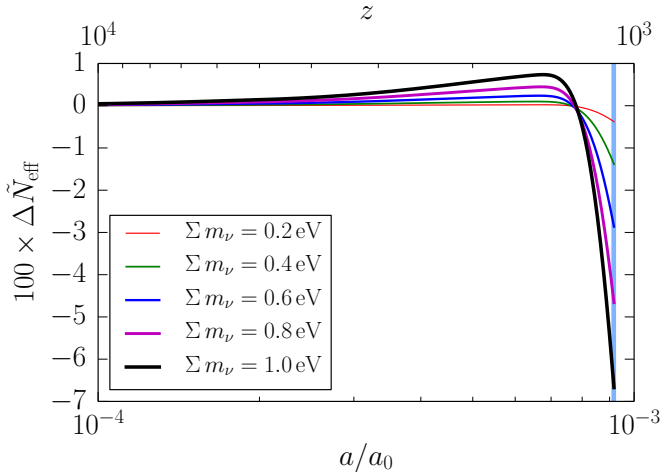


FIG. 5: (Color online.) The change in  $\tilde{N}_{\text{eff}}$ ,  $\Delta\tilde{N}_{\text{eff}}$ , is given as a function of scale factor ratio,  $a/a_0$ , and redshift,  $z$ , (at top). The primordial helium mass fraction and vertical bar are identical to Fig. 1. For each value of  $\sum m_\nu$ ,  $\Delta\tilde{N}_{\text{eff}}$  is initially positive.  $\Delta\tilde{N}_{\text{eff}}$  becomes negative once the recombination histories of Fig. 2 differ from the massless case.



we can examine the dependence of ionization freeze-out (and subsequent alteration of  $\tilde{N}_{\text{eff}}$ ) on both  $\sum m_\nu$  and  $Y_P$  simultaneously. A direct way to vary  $Y_P$  is to consider changes to the baryon number  $\omega_b$ . In the range of values of  $\omega_b$  that we're interested in,  $Y_P$  is a monotonically increasing function of  $\omega_b$ .

Figure 6 shows a contour plot of  $\Delta\tilde{N}_{\text{eff}}$  in the  $\sum m_\nu$  versus  $\omega_b$  parameter space; contours correspond to constant values of  $-\Delta\tilde{N}_{\text{eff}}$ . Varying  $\omega_b$  requires new computations of  $Y_P$  from BBN and  $X_e(a)$  from recombination. Changing  $\sum m_\nu$  requires a new computation of  $X_e$  but no new computation of  $Y_P$ . As a consequence, we compute BBN with the BURST code only once for a given  $\omega_b$ , and compute the recombination history for each pair  $(\omega_b, \sum m_\nu)$ . Holding  $\sum m_\nu$  fixed, the change in  $|\Delta\tilde{N}_{\text{eff}}|$  increases with increasing  $\omega_b$  due to the different recombination histories effecting a change in  $r_d$ . Note that the change in  $r_s$  does not completely compensate for the change in  $r_d$ . The shaded vertical region in Fig. 6 is the  $1\sigma$  range of  $\omega_b$  given by Ref. [11], but we explore a larger range in the  $\omega_b$  parameter space to illustrate the dependence of  $\tilde{N}_{\text{eff}}$  on  $\sum m_\nu$  and  $\omega_b$ . An interesting feature of these curves is their increasing curvature with decreasing  $\omega_b$  and increasing  $\sum m_\nu$ . This is a consequence of an enhancement of the  $\nu\text{MR}$  effect with increasing  $\omega_b$ : as  $\sum m_\nu$  increases, the change in  $\tilde{N}_{\text{eff}}$  is faster for higher values of  $\omega_b$ .

We have discussed two ways in which neutrino rest mass affects measurable quantities at photon decoupling. First, neutrino rest mass drives an earlier recombination freeze-out resulting in a higher free-electron fraction. Second, this effect is enhanced with increasing  $\omega_b$  stemming from a self-consistently calculated recombination history. As radiation energy density is not a directly

measurable quantity, we use observable quantities to indirectly arrive at the radiation energy density. For this purpose, we choose the ratio of the sound horizon to the photon diffusion length. Photon diffusion is sensitive to the recombination history, which requires a Boltzmann-equation treatment. We find a non-trivial evolution of  $\Delta\tilde{N}_{\text{eff}}$  with scale factor, as shown in Fig. 5. Note that the evolution of  $\tilde{N}_{\text{eff}}$  shown in this figure does not reflect a *kinematical* evolution of the radiation energy density with a massive component. The trends evidenced in this figure are a consequence of the  $\nu\text{MR}$  effect.

Self-consistency is a primary motivation for defining the radiation energy density parameter  $\tilde{N}_{\text{eff}}$  in terms of the ratio  $r_s/r_d$ ; it generalizes the  $N_{\text{eff}}^{(\text{th})}$  parameter to the massive neutrino case. Further,  $\tilde{N}_{\text{eff}}$  is defined for general energy densities and non-equilibrium distribution functions where the neutrino temperature is undefined. Moreover,  $\tilde{N}_{\text{eff}}$  makes no assumption regarding the underlying cosmological model. We use  $\tilde{N}_{\text{eff}}$  to relate the sound horizon and photon diffusion length to predictions made by the standard cosmological model via the parameter  $N_{\text{eff}}^{(\text{th})}$ .

The  $\nu\text{MR}$  effect is an example of a recurring phenomenon in cosmology: an increase in the expansion rate leads to an earlier epoch of freeze-out. This effect was revealed in the present context by using  $\tilde{N}_{\text{eff}}$  to *infer* the cosmic radiation energy content from observable CMB data, rather than treating  $N_{\text{eff}}^{(\text{th})}$  as an *input*. The procedure we describe here differs from that adopted by the public Boltzmann codes. CAMB[9], for example, includes options to evolve massive neutrino energy density through the epoch of recombination and requires  $N_{\text{eff}}^{(\text{th})}$  to be provided as an input.

Depending on  $\sum m_\nu$ , the concomitant changes in ionization equilibrium and  $\tilde{N}_{\text{eff}}$  discussed here may be within the sensitivity of the next generation CMB experiments when polarization effects are taken into account[11, 24–26]. CMB precision is planned to be increased to the  $\tilde{N}_{\text{eff}} \sim 1\%$  level which would probe both massive active neutrinos and other possible components of dark radiation. Scenarios with sterile neutrinos and other very weakly coupled light massive species with masses larger than those associated with the active neutrinos could enhance the effects discussed here. However, depending on their masses and their flavor mixing with active species, sterile neutrinos could have number densities and energy spectra which differ from those of active neutrinos [27–32], complicating the analysis given here.

We would like to acknowledge the Institutional Computing Program at Los Alamos National Laboratory for use of their HPC cluster resources. This work was supported in part by NSF grant PHY-1307372 at UC San Diego, by the Los Alamos National Laboratory Institute for Geophysics, Space Sciences and Signatures sub-contract 257842, and the National Nuclear Security Ad-

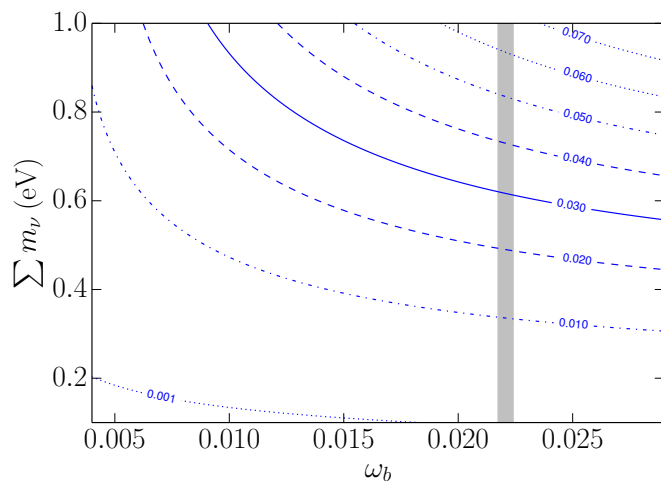


FIG. 6: (Color online.) Contours of constant  $-\Delta\tilde{N}_{\text{eff}}$  in the  $\sum m_\nu$  vs.  $\omega_b$  parameter space. The shaded, vertical bar corresponds to the  $1\sigma$  error for  $\omega_b$  [11].

ministration of the U.S. Department of Energy at Los Alamos National Laboratory under Contract No. DE-AC52-06NA25396. We thank J.J. Cherry, Amit Yadav, and Lloyd Knox for helpful discussions. We would also like to thank the anonymous referees for their useful comments.

- 
- [1] A. D. Dolgov, S. H. Hansen, and D. V. Semikoz, Nucl. Phys. B **543**, 269 (1999), hep-ph/9805467.
  - [2] J.-L. Cambier, J. R. Primack, and M. Sher, Nucl. Phys. B **209**, 372 (1982).
  - [3] R. E. Lopez and M. S. Turner, Phys. Rev. D **59**, 103502 (1999), astro-ph/9807279.
  - [4] G. Mangano, G. Miele, S. Pastor, and M. Peloso, PLB **534**, 8 (2002), astro-ph/0111408.
  - [5] M. Shimon, N. J. Miller, C. T. Kishimoto, C. J. Smith, G. M. Fuller, and B. G. Keating, J. Cosmology Astropart. Phys. **5**, 037 (2010), 1001.5088.
  - [6] Z. Hou, R. Keisler, L. Knox, M. Millea, and C. Reichardt, Phys. Rev. D **87**, 083008 (2013), 1104.2333.
  - [7] J. Birrell, C.-T. Yang, P. Chen, and J. Rafelski, Phys. Rev. D **89**, 023008 (2014).
  - [8] Z. Hou, C. L. Reichardt, K. T. Story, B. Follin, R. Keisler, K. A. Aird, B. A. Benson, L. E. Bleem, J. E. Carlstrom, C. L. Chang, et al., ApJ **782**, 74 (2014), 1212.6267.
  - [9] C. Howlett, A. Lewis, A. Hall, and A. Challinor, JCAP **1204**, 027 (2012), 1201.3654.
  - [10] J. Lesgourgues and S. Pastor, Adv. High En. Phys. **2012**, 608515 (2012), 1212.6154.
  - [11] Planck Collaboration, A&A **571**, A16 (2014), 1303.5076.
  - [12] W. Hu and N. Sugiyama, ApJ **471**, 542 (1996), astro-ph/9510117.
  - [13] P. J. E. Peebles, ApJ **153**, 1 (1968).
  - [14] Y. B. Zeldovich, V. G. Kurt, and R. A. Syunyaev, Zhurnal Eksperimentalnoi i Teoreticheskoi Fiziki **55**, 278 (1968).
  - [15] S. Seager, D. D. Sasselov, and D. Scott, ApJ **523**, L1 (1999), astro-ph/9909275.
  - [16] O. Zahn and M. Zaldarriaga, Phys. Rev. D **67**, 063002 (2003).
  - [17] G. Mangano, G. Miele, S. Pastor, T. Pinto, O. Pisanti, and P. D. Serpico, Nuclear Physics B **729**, 221 (2005), hep-ph/0506164.
  - [18] E. Grohs, G. M. Fuller, C. T. Kishimoto, and M. W. Paris, J. Cosmology Astropart. Phys. **5**, 17 (2015), 1502.02718.
  - [19] G. M. Fuller and C. T. Kishimoto, Phys. Rev. Lett. **102**, 201303 (2009), 0811.4370.
  - [20] A. D. Dolgov, M. V. Sazhin, and Y. B. Zeldovich, *Basics of modern cosmology* (1990).
  - [21] Y. I. Izotov and T. X. Thuan, ApJ **710**, L67 (2010).
  - [22] E. Aver, K. A. Olive, R. L. Porter, and E. D. Skillman, J. Cosmology Astropart. Phys. **11**, 017 (2013), 1309.0047.
  - [23] A. D. Dolgov et al., Nucl. Phys. B **632**, 363 (2002), hep-ph/0201287.
  - [24] K. Abazajian et al., Astroparticle Physics **63**, 66 (2015), ISSN 0927-6505.
  - [25] The Polarbear Collaboration: P. A. R. Ade et al., ApJ **794**, 171 (2014), 1403.2369.
  - [26] J. E. Carlstrom and Spt Collaboration, IAU Special Session **2**, 34 (2003).
  - [27] K. Abazajian, N. F. Bell, G. M. Fuller, and Y. Y. Y. Wong, Phys. Rev. D **72**, 063004 (2005), astro-ph/0410175.
  - [28] C. T. Kishimoto, G. M. Fuller, and C. J. Smith, Phys. Rev. Lett. **97**, 141301 (2006), astro-ph/0607403.
  - [29] J. Hamann, S. Hannestad, G. G. Raffelt, I. Tamborra, and Y. Y. Y. Wong, Phys. Rev. Lett. **105**, 181301 (2010), 1006.5276.
  - [30] J. Hamann, S. Hannestad, G. G. Raffelt, and Y. Y. Y. Wong, J. Cosmology Astropart. Phys. **9**, 034 (2011), 1108.4136.
  - [31] C. Dvorkin, M. Wyman, D. H. Rudd, and W. Hu, Phys. Rev. D **90**, 083503 (2014), 1403.8049.
  - [32] M. Cirelli, G. Marandella, A. Strumia, and F. Vissani, Nuclear Physics B **708**, 215 (2005), hep-ph/0403158.